Results in Physics 56 (2024) 107246

Contents lists available at ScienceDirect

Results in Physics

journal homepage: www.elsevier.com/locate/rinp

Dzyaloshinskii-Moriya bias in a free-standing asymmetric homogeneous nanodisk

S. Castillo-Sepúlveda [a], R.M. Corona [b,f], M. Kiwi [c,f], V.L. Carvalho-Santos [d,f], D. Altbir [e,f,*]

[a] Grupo de Investigación en Física Aplicada, Facultad de Ingeniería, Universidad Autónoma de Chile, Avda. Pedro de Valdivia 425, Providencia, Chile
[b] Departamento de Física, Facultad de Ciencias Naturales, Matemática y del Medio Ambiente, Universidad Tecnológica Metropolitana, Las Palmeras 3360, Ñuñoa 780-0003, Santiago, Chile
[c] Departamento de Física, Facultad de Ciencias, Universidad de Chile, Las Palmeras 3425, Ñuñoa, Santiago, 7571468, Chile
[d] Universidade Federal de Viçosa, Departamento de Física, Avenida Peter Henry Rolfs s/n, 36570-000, Viçosa, MG, Brazil
[e] Universidad Diego Portales, Ejército 441, Santiago, Chile
[f] Centro para el Desarrollo de la Nanociencia y la Nanotecnología, CEDENNA, Av. Libertador Bernardo O'Higgins 3363, 9170124, Santiago, Chile

ARTICLE INFO

Keywords:
Dzyaloshinskii-Moriya (DM) interaction
Magnetochirality
Bias
Asymmetric nanoparticles
Magnetization reversal

ABSTRACT

An off-center shift of the magnetic hysteresis loop, usually known as exchange bias, develops in an asymmetric nanodisk due to the Dzyaloshinskii-Moriya (DM) interaction. Results exhibit the onset of bias in a system without material interfaces, originating from the relation between the chirality defined by the DM interaction and the geometry. In addition, programmable magnetization bias by the variation of an external field emerges as a possibility. Our simulations, carried out using Mumax3 code, also yield double hysteresis loops, evidencing a magnetization reversal driven by vortex nucleation and annihilation. Bias in a homogeneous nanodisk and its control seem promising for applications.

The physics of magnetic structures in low-dimensional systems have attracted significant attention in recent years [1–5]. This interest is based on the properties such nanostructures exhibit and their potential for different applications [6–10]. An interesting phenomenon in magnetic systems at the nanoscale is biased hysteresis loops. This bias has been usually associated with exchange or dipolar interactions and is known as exchange (EB) or dipolar bias (DB) [11–13].

Several bias mechanisms have already been explored. For example, a quantum mechanical approach to EB was developed by Suhl and Schuller [14] based on interactions of spins across the FM-AFM interface, which causes an energy shift of the hysteresis loop. Another example is the dipole-induced EB, presented by Torres et al. [13], who described experimental results in systems where a paramagnetic spacer separates the AFM and the FM. The dipole field originates in quantum fluctuations of frustrated spins in the AFM, which breaks the balance between the two AFM sublattices. From the applied point of view, Kim et al. [15] implemented programmable exchange bias by controlling magnetic domain wall motion dynamics in multilayer systems. To our knowledge, all published EB work since Meiklejohn and Bean discovered the phenomenon [16,17], relies on interface interactions to generate EB.

Focusing on dipolar interactions, Allende et al. [18] investigated asymmetric magnetization loops in multilayered nanowires and obtained different reversal modes, which appear due to dipolar interactions along the wire. Popov [19] analytically studied the bi-domain configuration of cylindrical magnetic micro-particles and estimated the dependence of the inner domain dimensions on bias magnetic field and direction. Pitzschel et al. [20] explored bias in multilayered $Fe_3O_4/ZrO_2/Fe_3O_4$ nanotubes (that is, a ferromagnetic (FM) internal tube, an intermediate non-magnetic spacer, and an external magnetic shell). Using a continuum approach, analytical expressions were obtained that support their interpretation of the experiment as the behavior of two isolated magnetic systems. Sinnecker et al. [21] studied the effect of the dipolar field on the magnetoimpedance in Fe- and Co-based nanowires, where the Co wire was used as a probe for the magnetoimpedance, and the Fe wire generated the dipolar field. They found that the magnetoimpedance shifted in the anisotropy field but kept a highly asymmetric profile. Lu and Hu [22] used Monte Carlo to study DB, including short-range exchange, anisotropy, and long-range dipolar interactions, to study the temperature dependence of DB. They highlighted the role of the antiferromagnet (AFM) magnetization and stressed that the dipolar interaction incorporates the AFM bulk magnetization as a relevant player that yields non-contact bias. All these

* Corresponding author at: Universidad Diego Portales, Ejército 441, Santiago, Chile.
E-mail address: dora.altbir@udp.cl (D. Altbir).

https://doi.org/10.1016/j.rinp.2023.107246
Received 22 August 2023; Received in revised form 20 November 2023; Accepted 3 December 2023
Available online 5 December 2023

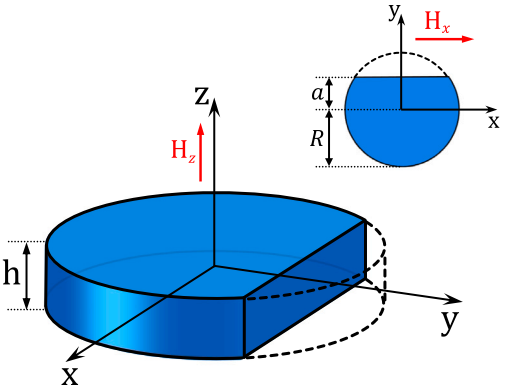

Fig. 1. Schematic representation of our asymmetric disk, illustrating the parameters a, R and h. The inset is the top view of the structure.

systems are formed by two or more subsystems, and the interaction between them is the mechanism to generate the bias.

Previously [23–25], the chirality C, and polarity P, of a vortex nucleated during the reversal process in an asymmetric non-chiral nanodisk was examined. It was concluded that the vortex chirality and the nucleation regions depend on the disk asymmetry (vortex nucleation onset is observed near the straight "cut" of Fig. 1). However, in those cases, symmetric hysteresis loops were always obtained. If a bulk Dzyaloshinskii-Moriya interaction (DMI) [26–28] is included, and due to the chirality associated with the DMI, one expects that the states that appear during the magnetization reversal depend on the interplay between the chirality induced by the nanodisk asymmetry and bulk DMI. Using this effect, we present a way to generate bias in a free-standing homogeneous nanosystem without interfaces: a nanodisk, as illustrated in Fig. 1. Our results show a shift in the hysteresis loop of such a system. However, in contrast to previous works, the onset of bias is not due to interfacial interactions but materializes due to the system asymmetry plus the DMI. From now on, this bias will be called the Dzyaloshinskii-Moriya bias (DMB). The existence of a bias without interface interactions opens novel roads to explore nanosized systems and their eventual technological uses, such as programmable DM bias, by controlling the strength of an external magnetic field.

Model: Our system is a uniform disk, $R = 40$ nm in radius and a height $h = 30$ nm. The asymmetry is created through a cut parallel to the disk axis at a distance a from its center, as shown in Fig. 1. The parameter to characterize the asymmetry is defined as $\beta = a/R$. This way, a half disk is obtained when $\beta = 0.0$, and a full disk corresponds to $\beta = 1.0$. In the calculations, we make use of typical parameters for chiral ferromagnets [29,30]; that is, an exchange constant $A = 15\times10^{-12}$ J/m, a saturation magnetization $M_s = 0.58\times10^{6}$ A/m, and a Gilbert damping constant $\alpha = 0.001$. The DMI constant D we adopted is in the range $0 \le D \le 10^{-3}$ J/m^2, which favors a counterclockwise chirality due to its positive sign.

The magnetization dynamics is governed by the Landau–Lifshitz–Gilbert equation

$$\frac{d\vec{\mathbf{m}}}{dt} = -\gamma\vec{\mathbf{m}}\times\vec{\mathbf{H}}_{\text{eff}} + \alpha\left(\vec{\mathbf{m}}\times\frac{d\vec{\mathbf{m}}}{dt}\right), \tag{1}$$

where γ is the gyromagnetic ratio and the normalized magnetization $\vec{\mathbf{m}}$ is defined as $\vec{\mathbf{m}} = \vec{\mathbf{M}}/M_s$, $\vec{\mathbf{H}}_{\text{eff}} = -(1/\mu_0 M_s)\delta E/\delta\vec{\mathbf{m}}$ is the effective field, $E = E_{ex} + E_d + E_{DM} + E_Z$ is the total energy density, given by:

$$\begin{aligned} E_{ex} &= A[(\vec{\nabla}m_x)^2 + (\vec{\nabla}m_y)^2 + (\vec{\nabla}m_z)^2], \\ E_d &= \frac{1}{2}\mu_0 M_s(\vec{\mathbf{m}}\cdot\vec{\nabla}U), \\ E_{DM} &= D\vec{\mathbf{m}}\cdot(\vec{\nabla}\times\vec{\mathbf{m}}), \\ E_Z &= \mu_0\vec{\mathbf{m}}\cdot\vec{\mathbf{H}}, \end{aligned} \tag{2}$$

where

$$U = \frac{1}{4\pi}\oint_S \frac{\vec{\mathbf{n}}'\cdot\vec{\mathbf{m}}'}{|\vec{\mathbf{r}}'-\vec{\mathbf{r}}|}\,dA' - \frac{1}{4\pi}\int_V \frac{\vec{\nabla}'\cdot\vec{\mathbf{n}}'}{|\vec{\mathbf{r}}'-\vec{\mathbf{r}}|}\,dV',$$

and E_{ex}, E_d, E_{DM}, and E_Z are respectively the exchange, dipolar, Dzyaloshinskii-Moriya, and Zeeman contributions to the total energy density.

Results: Our approach uses simulation techniques to obtain the magnetic structure properties. These simulations are performed using the Mumax3 package [31,32] and cells of size $2 \times 2 \times 2$ nm^3 are adopted. The DMI contribution is calculated for three different values of D: 0.5, 0.75, and 1.0 mJ/m^2. The applied magnetic field has two components

$$\vec{\mathbf{H}} = \vec{\mathbf{H}}_z + \vec{\mathbf{H}}_x\,, \tag{3}$$

where $\vec{\mathbf{H}}_z = \hat{\mathbf{z}}\,\mathrm{H}_z$ is a constant external magnetic field, and $\vec{\mathbf{H}} = \hat{\mathbf{x}}\,\mathrm{H}_x$, is the measurement field to obtain the hysteresis loop. H is swept in $\Delta\mathrm{H}_x = -10$ Oe steps, from 3000 Oe to −3000 Oe, and increased in a similar fashion. These field values are chosen to ensure saturation at both extremes of the magnetization cycles. The initial magnetic configuration is always $\vec{\mathbf{m}} = m\hat{\mathbf{x}}$, and we have evaluated $\vec{\mathbf{m}}$ for each H-value. To characterize each simulation, three model parameters defined above β, D, H_z are required.

Mechanisms that govern the magnetization loop asymmetries: Figs. 2 and 3 display the asymmetries of the magnetization *vs* applied field, which is absent for $\mathrm{H}_z = 0$, as expected. In particular, the emergence of negative bias is quite apparent, both for the axial $\vec{\mathbf{m}}_\mathbf{z}$ and transverse $\vec{\mathbf{m}}_\mathbf{x}$ directions.

The behavior of the x-component of the magnetization indicates that the reversal occurs through two main mechanisms: a quasi-coherent-rotation, evidenced by the single magnetization cycle presented in Fig. 2 and the nucleation and propagation of a vortex, as shown in Fig. 3, where a double magnetization cycle is observed. As it will be shown after, the range in which the vortex persists is largely controlled by the H_z field. The asymmetry of the magnetization loops is due to a competition between the energies specified in Eq. (2). These results suggest the existence of a critical value in which the quasi-coherent-rotation reversion gives place to a reversal process mediated by a spin vortex configuration, whose value is $\beta = 0.6$ for the geometry considered in the paper. However, vortex nucleation requires a minimum volume. Therefore, in larger disks, a vortex can nucleate at lower β values. On the contrary, smaller disks require larger β to increase the dipolar energy required to nucleate a vortex.

First we analyze the reversal process mediated by vortex nucleation, where asymmetric double hysteresis loops are observed. This is quite remarkable since usually such behavior has been attributed to a FM/AFM bilayer breakup into a bi-domain state, with staggered FM/AFM regions of opposite uncompensated moments in the AFM layer [33,34]. Brück et al. [35] suggested that these structures are due to the imprinting of the domain pattern of the FM into the AFM during zero-field cooling. Our results suggest that they are a more general phenomenon. The analysis of Fig. 3(b) also shows that the vortex core direction and how it depends on H_z, evidencing that, depending on β and H_z, a change of polarity occurs.

When the DM and the Zeeman terms are absent ($D = 0.0$ and $\mathrm{H}_z = 0$), the competition between exchange and dipolar energies forces the formation of vortices. They nucleate in the region that requires the least energy, and the most favorable zone for them to emerge is in the vicinity of the disk straight cut [24,25]. As expected, it is observed that the vortex propagates perpendicular to the applied field.

The vortex is characterized by its helicity ($C = +1$ for clockwise and $C = -1$ for counterclockwise swirling), which is determined by the direction of the initial magnetization $\vec{\mathbf{m}}_x$. Also, the vortex has a polarity P, defined as $+1$ (-1) when the vortex core points along $+\hat{\mathbf{z}}$ ($-\hat{\mathbf{z}}$). In dots without DMI, the polarity is undetermined [25], with a

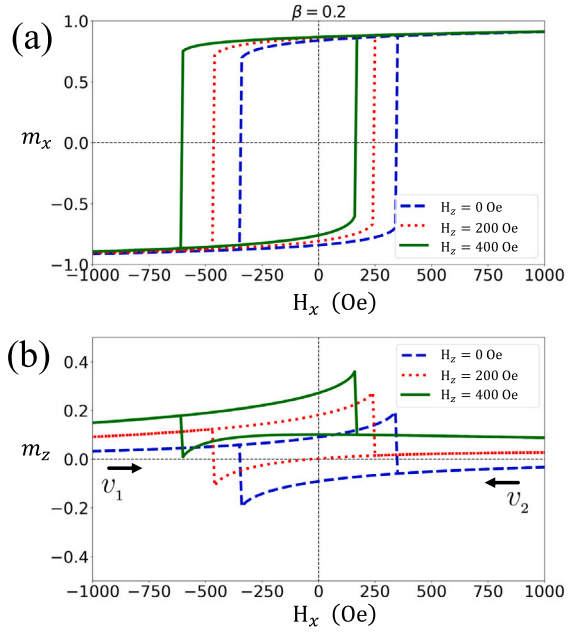

Fig. 2. m_x (top) and m_z (bottom) for $D = 1.0$ mJ/m^2 and $\beta = 0.2$, for several values of H$_z$.

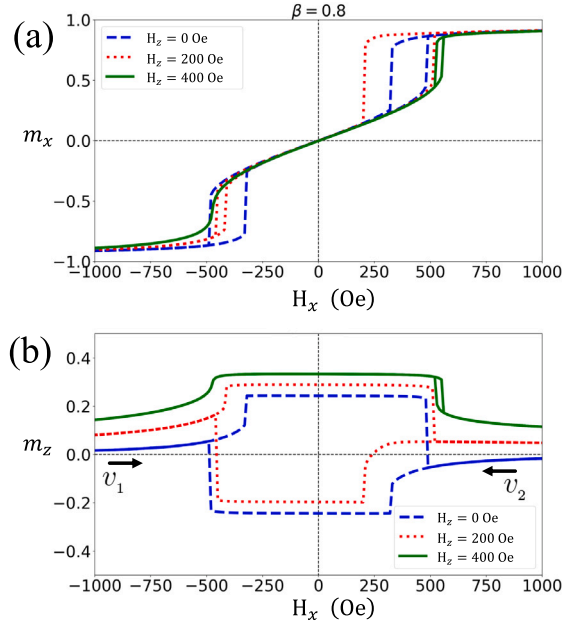

Fig. 3. m_x (top) and m_z (bottom) for m_x (top) and m_z (bottom) for $D = 1.0$ mJ/m^2 and $\beta = 0.8$, for several values of H$_z$.

random probability of $P = \pm 1$ for any helicity value. But, when the DMI is included, there is a coupling between helicity and polarity, with the latter being determined by the magnetization swirling; for positive values of D and $C = -1$, the lower energy state corresponds to $P = -1$, while the higher one is associated with $P = +1$. In other words, adding the DMI implies well-defined polarity, ensuring the product $CP = -1$.

When a magnetic field, $\hat{\mathbf{H}}_z$, is applied parallel to $+\hat{\mathbf{z}}$, the situation becomes more complex as the vortex core tends to align with the external field, leading to a competition between DMI and Zeeman energies. In fact, when H$_z$ is less than a critical field value $H_z^{(c)}$, the core can point along $\pm\hat{\mathbf{z}}$, and a vortex nucleates in the low-energy region, as shown in snapshots 1 and 2 (for $\mathbf{H}_x$ varying from $+\hat{\mathbf{x}}$ to $-\hat{\mathbf{x}}$), and 3 and 4

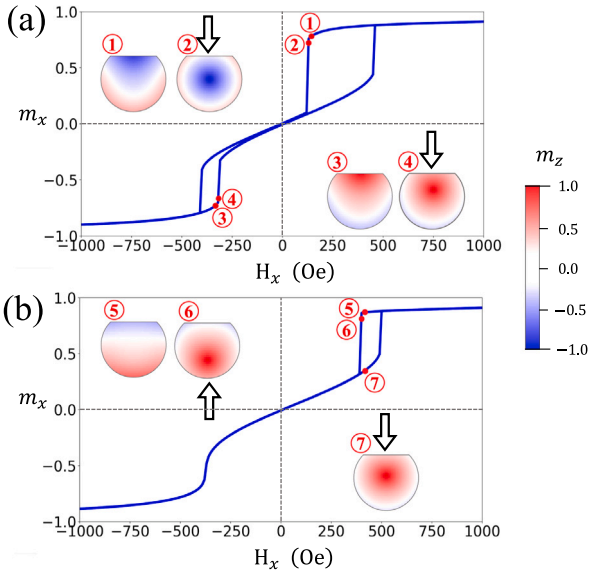

Fig. 4. (a) Reversal mechanism for H$_z$ <H$_z^c$, and (b) H$_z$ >H$_z^c$. A blue vortex corresponds to $C = +1$ and $P = -1$, while a red core illustrates the $C = -1$ and $P = +1$ case. The vortex core for $P = +1$ is aligned with $\vec{\mathbf{H}}_z$, while for $P = -1$ it is anti-parallel. Arrows illustrate the region where the vortex nucleate. (For interpretation of the references to color in this figure legend, the reader is referred to the web version of this article.)

(for $\mathbf{H}_x$ varying from $-\hat{\mathbf{x}}$ to $+\hat{\mathbf{x}}$) of Fig. 4(a). In this case, the nucleation of a vortex in the vicinity of the cut allows the product CP to minimize the DMI. When $H_z > H_z^{(c)}$ the polarity can only be oriented along $\vec{\mathbf{H}}_z$, and therefore, to minimize the DMI, a vortex is nucleated in the high energy zone, with clockwise helicity, as depicted in snapshots 5 and 6 of Fig. 4(b). This is the reason for the asymmetry of the magnetization cycles and the consequent onset of DMB.

All in all, the loop asymmetry is understood as due to the competition between the different magnetic energies of the system. We have checked that generating vortices is a general feature of asymmetric disks, even with no sharp corners.

Effects due to the variation of H$_z$: Now we focus on the magnetization reversal mechanisms. The vortex core presents two polarities depending on H$_z$. To develop an insight on this issue, we define Δ as $|H_n - H_a|$, where H$_n$ (H$_a$) correspond to the vortex nucleation (annihilation) fields. This field range is related to the vortex persistence as a function of an applied field H$_x$ aligned parallel to the x-axis, as illustrated in Fig. 5. Open symbols represent Δ when H$_x$ is decreased from saturation along the $+\hat{\mathbf{x}}$ to the $-\hat{\mathbf{x}}$ direction, (a path which we define as υ_1); the full symbols represent the reverse process, that is, the increase of H$_x$ from saturation along $-\hat{\mathbf{x}}$ to the $+\hat{\mathbf{x}}$ direction (defined as υ_2). Results show that the vortex persists over a larger range when propagating according to υ_1 compared to υ_2. Moreover, when the υ_1 path is followed, there is a change in the slope in Δ_1, reflecting a polarity change at the critical field H_z^c, which depends on the β value, as shown in Fig. 5(b). This behavior emerges due to the competition between the Zeeman and DMI interactions. When $H_z = 0$, υ_1 and υ_2 lead to equivalent results, as expected.

Quasi-coherent rotation reversal mechanism: As mentioned above, depending on the physical parameters of the system, it is possible to reverse the magnetization through a quasi-coherent rotation, in which the magnetic moments rotate almost simultaneously around the nanodisk axis. This reversal occurs for small β since the disk does not have enough surface to nucleate a vortex. It is characterized by an almost square magnetization cycle [25], as shown in Fig. 2(a), where we present the magnetization cycles for $\beta = 0.2$. In this case, the asymmetry in the magnetization loops increases as a function of H$_z$.

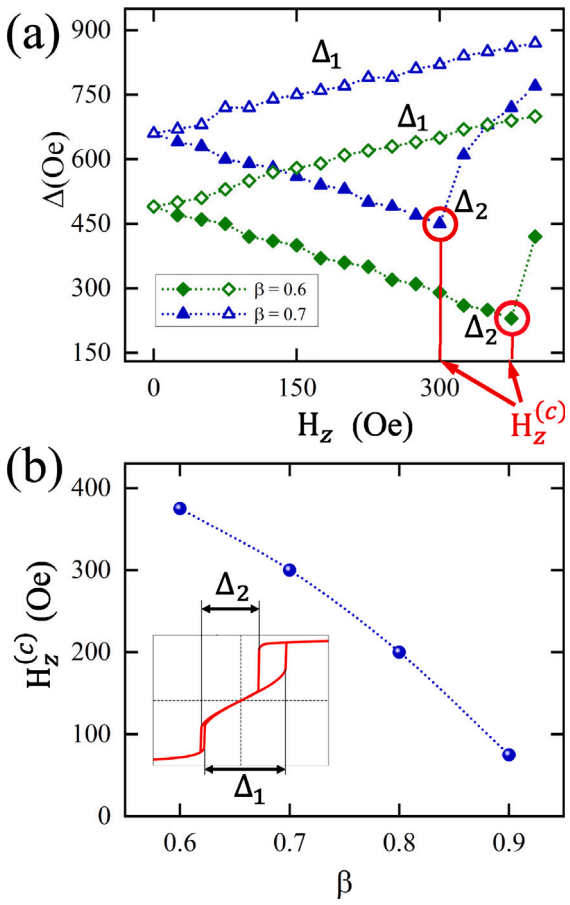

Fig. 5. (a) $\Delta = |H_n - H_a|$, for $\beta = 0.6$ and $\beta = 0.7$. Full symbols represent the trajectory v_1, while open symbols correspond to v_2. (b) H_z^c as a function of β. The inset presents a visualization of Δ_1 and Δ_2 in the magnetization cycle.

Although the quasi-coherent rotation is not characterized by polarity and helicity, there is also a small magnetization component along the **z**-axis. Therefore, because the magnetic moments in the straight nanodisk surface experience a lower exchange interaction, they facilitate the formation of a state where the in-plane component of the magnetization presents a slight deviation from the parallel configuration, forming a C-like pattern [25]. In this context, the DMI establishes a coupling between the $\mathbf{m}_z$ and the rotation direction of the in-plane deviation. Again, the presence of H_z forces the out-of-plane component to point along the +**z**-direction, and the DMI minimization leads to asymmetric magnetization loops, allowing H_z to control the DM bias.

The realization of programmable magnetic bias for applications was proposed by Kim et al. [15], who implemented programmable exchange bias by controlling magnetic domain wall motion in multilayer systems. Controllable bias is a very desirable feature for applications. Here, we put forward an alternative: control the shift of the hysteresis loop in a nanosystem without neither interfaces nor domain walls by varying an externally applied magnetic field.

Conclusions: In this paper, we developed a model calculation of the magnetic properties of free-standing homogeneous asymmetric nanodisks. The model incorporates exchange, dipolar and Dzyaloshinskii-Moriya interactions and the simulations were carried out using the Mumax3 package. On this basis, we obtain a novel result: bias in a free-standing homogeneous system without physical interfaces. At the same time, double hysteresis loops are obtained, which suggests that the mechanism that generates them is by vortex nucleation and annihilation. Moreover, programmable magnetic bias, controlled by an applied field, emerges as a possibility.

The fact that in a free-standing asymmetric homogeneous nanodisk magnetic bias materializes, opens interesting prospects for applications.

CRediT authorship contribution statement

S. Castillo-Sepúlveda: Conceptualization, Software, Writing – original draft. **R.M. Corona:** Conceptualization, Software, Writing – original draft. **M. Kiwi:** Conceptualization, Supervision, Writing – original draft. **V.L. Carvalho-Santos:** Conceptualization, Investigation, Methodology, Writing – original draft. **D. Altbir:** Conceptualization, Investigation, Writing – review & editing.

Declaration of competing interest

The authors declare that they have no known competing financial interests or personal relationships that could have appeared to influence the work reported in this paper.

Data availability

Data will be made available on request.

Acknowledgments

This work was supported by CEDENNA through Financiamiento Basal para Centros Científicos y Tecnológicos de Excelencia (grant AFB220001). We also acknowledge support from FONDECYT, Chile under Projects #1211902. and 1220215. CNPq, Brazil (Grant No. 305256/2022), and Fapemig, Brazil (Grant No. APQ-00648-22). V.L.C-S acknowledges Universidad de Santiago de Chile and CEDENNA for hospitality.

References

[1] Stamopoulos D. Magnetism and superconductivity in low-dimensional systems: Utilization in future applications. Nova Science Pub Inc; UK ed.; 2008.
[2] Blügel S, Bihlmayer G. Magnetism of low-dimensional systems: Theory. In: Handbook of magnetism and advanced magnetic materials. John Wiley & Sons, Ltd; 2007.
[3] Regnault L-P. Bulk magnetic materials: Low-dimensional systems. In: Buschow KJ, Cahn RW, Flemings MC, Ilschner B, Kramer EJ, Mahajan S, Veyssière P, editors. Encyclopedia of materials: science and technology. Oxford: Elsevier; 2001, p. 856–64.
[4] Katsumata K. Low-dimensional magnetic materials. Curr Opin Solid State Mater Sci 1997;2(2):226–30.
[5] Gupta R, Mishra S, Nguyen T. Fundamentals of low dimensional magnets. 1st ed.. CRC Press; 2022.
[6] Hirohata A, Yamada K, Nakatani Y, Prejbeanu I-L, Diény B, Pirro P, et al. J Magn Magn Matter 2020;509:166711.
[7] Hrkac G, Dean J, Allwood DA. Philos Trans R Soc A 2011;369:3214.
[8] Vandermeulen J, de Wiele BV, Dupré L, Waeyenberge BV. J Phys D: Appl Phys 2015;48:275003.
[9] Torrejon J, Riou M, Araujo FA, Tsunegi S, Khalsa G, Querlioz D, et al. Nature 2017;547:428.
[10] Grollier J, Querlioz D, Camsari KY, Everschor-Sitte K, Fukami S, Stiles MD. Nat Electron 2020;3:360.
[11] Nogues J, Schuller IK. Exchange bias. J Magn Magn Mater 1999;192:203.
[12] Kiwi M. Exchange bias theory. J Magn Magn Mater 2001;234/3:584.
[13] Torres F, Morales R, Schuller IK, Kiwi M. Dipole-induced exchange bias. Nanoscale 2017;9:17074.
[14] Suhl H, Schuller IK. Spin-wave theory of exchange-induced anisotropy. Phys Rev B 1998;58:258.
[15] Kim H-J, Je S-G, Moon K-W, Choi W-C, Yang S, Kim C, et al. Programmable dynamics of exchange-biased domain wall via spin-current-induced antiferromagnet switching. Adv Sci 2021;8(17):2100908.
[16] Meiklejohn WH, Bean CP. New magnetic anisotropy. Phys Rev 1956;102:1413.
[17] Meiklejohn WH, Bean CP. New magnetic anisotropy. Phys Rev 1957;105:904.
[18] Allende S, Escrig J, Altbir D, Salcedo E, Bahiana M. Asymmetric hysteresis loop in magnetostatic-biased multilayer nanowires. Nanotechnology 2009;20:445707.
[19] Popov MA. Equilibrium bi-domain configuration in cylindrical magnetic microparticles. Eur Phys J 2017;B90:55.

[20] Pitzschel K, Bachmann J, Montero-Moreno J, Escrig J, Gorlitz D, Nielsch K. Reversal modes and magnetostatic interactions in Fe3O4/ZrO2/Fe3O4 multilayer nanotubes. Nanotechnology 2012;23:495718.
[21] Sinnecker J, de Araujo A, Piccin R, Knobel M, Vázquez M. Dipolar-biased giant magnetoimpedance. J Magn Magn Mater 2005;295:121.
[22] Lu Q, Hu Y. Temperature dependence of dipole-induced exchange bias. Nanotechnology 2012;31:305703.
[23] Castillo-Sepúlveda S. Appearance of stagnation points in skyrmion-based STNO due to geometric asymmetries. J Magn Magn Mater 2020;503:166589.
[24] Leighton B, Vargas NM, Altbir D, Escrig J. Tailoring the magnetic properties of Fe asymmetric nanodots. J Magn Magn Mater 2011;323:1563.
[25] Vargas NM, Allende S, Leighton B, Escrig J, Mejía-López J, Altbir D, et al. J Appl Phys 2011;109:073907.
[26] Dzyaloshinskii IE. Thermodynamic theory of "Weak" ferromagnetism in antiferromagnetic substances. Sov Phys JETP 1957;5:1259.
[27] Moriya T. New mechanism of anisotropic superexchange interaction. Phys Rev Lett 1960;4:228.
[28] Moriya T. Anisotropic superexchange interaction and weak ferromagnetism. Phys Rev 1960;120:91.
[29] Huang SX, Chien CL. Extended skyrmion phase in epitaxial FeGe(111) thin films. Phys Rev Lett 2012;108:267201.
[30] Wang W, Albert M, Beg M, Bisotti M, Chernyshenko D, Cortés-Ortuño D, et al. Magnon-driven domain-wall motion with the Dzyaloshinskii-Moriya interaction. Phys Rev Lett 2015;114:087203.
[31] Vansteenkiste A, Leliaert J, Dvornik M, Helsen M, Garcia-Sanchez F, Van Waeyenberge B. The design and verification of Mumax3. AIP Adv 2014;4(10):107133.
[32] Vansteenkiste A, de Wiele BV. MuMax: A new high-performance micromagnetic simulation tool. J Magn Magn Mater 2011;323:2585.
[33] Morales R, Vélez M, Petracic O, Roshchin IV, Li Z-P, Batlle X, et al. Three-dimensional spin structure in exchange-biased antiferromagnetic/ ferromagnetic thin films. Appl Phys Lett 2009;95:092503.
[34] Jia J, Chen Y, Wang B, Han B, Wu Y, Wang Y, et al. The double-shifted magnetic hysteresis loops and domain structure in perpendicular [Co/Ni]N/IrMn exchange biased systems. J Phys D: Appl Phys 2018;52(6):065001.
[35] Brück S, Sort J, Baltz V, Suriñach S, Muñoz JS, Dieny B, et al. Adv Mater 2005;17:2978.